Autosomal-Recessive Hearing Impairment Due to Rare Missense Variants within *S1PR2*

Regie Lyn P. Santos-Cortez,[1,14] Rabia Faridi,[2,3,14] Atteeq U. Rehman,[2] Kwanghyuk Lee,[1] Muhammad Ansar,[1,4] Xin Wang,[1] Robert J. Morell,[2] Rivka Isaacson,[5] Inna A. Belyantseva,[2] Hang Dai,[1] Anushree Acharya,[1] Tanveer A. Qaiser,[3] Dost Muhammad,[6] Rana Amjad Ali,[7] Sulaiman Shams,[8] Muhammad Jawad Hassan,[9] Shaheen Shahzad,[10] Syed Irfan Raza,[4] Zil-e-Huma Bashir,[3] Joshua D. Smith,[11] Deborah A. Nickerson,[11] Michael J. Bamshad,[11] University of Washington Center for Mendelian Genomics, Sheikh Riazuddin,[7,12,13] Wasim Ahmad,[4] Thomas B. Friedman,[2] and Suzanne M. Leal[1,*]

The sphingosine-1-phosphate receptors (S1PRs) are a well-studied class of transmembrane G protein-coupled sphingolipid receptors that mediate multiple cellular processes. However, S1PRs have not been previously reported to be involved in the genetic etiology of human traits. *S1PR2* lies within the autosomal-recessive nonsyndromic hearing impairment (ARNSHI) locus *DFNB68* on 19p13.2. From exome sequence data we identified two pathogenic *S1PR2* variants, c.323G>C (p.Arg108Pro) and c.419A>G (p.Tyr140Cys). Each of these variants co-segregates with congenital profound hearing impairment in consanguineous Pakistani families with maximum LOD scores of 6.4 for family DEM4154 and 3.3 for family PKDF1400. Neither *S1PR2* missense variant was reported among ~120,000 chromosomes in the Exome Aggregation Consortium database, in 76 unrelated Pakistani exomes, or in 720 Pakistani control chromosomes. Both DNA variants affect highly conserved residues of S1PR2 and are predicted to be damaging by multiple bioinformatics tools. Molecular modeling predicts that these variants affect binding of sphingosine-1-phosphate (p.Arg108Pro) and G protein docking (p.Tyr140Cys). In the previously reported *S1pr2*$^{-/-}$ mice, stria vascularis abnormalities, organ of Corti degeneration, and profound hearing loss were observed. Additionally, hair cell defects were seen in both knockout mice and morphant zebrafish. Family PKDF1400 presents with ARNSHI, which is consistent with the lack of gross malformations in *S1pr2*$^{-/-}$ mice, whereas family DEM4154 has lower limb malformations in addition to hearing loss. Our findings suggest the possibility of developing therapies against hair cell damage (e.g., from ototoxic drugs) through targeted stimulation of S1PR2.

Sphingosine-1-phosphate (S1P) is one of the most studied sphingolipids due to its multiple roles in cellular proliferation, inflammation, migration, cytoskeletal organization, and angiogenesis that are mediated by either intracellular targets (e.g., class-I histone deacetylases) or one of five transmembrane G protein-coupled receptors (GPCRs), namely S1PR1–5.[1] Over the past 20 years, the tissue distribution of these five receptors and the phenotypes of knockout mice for each S1PR have been well documented,[1] such as vascular phenotypes for S1PR1,[2] deafness for S1PR2,[3–5] small litter size for S1PR3,[6] atypical megakaryocytes for S1PR4,[7] and lack of peripheral monocytes for S1PR5.[8] In humans, pathogenic variants have not been reported for any of the S1PRs.

Previously, the autosomal-recessive (ar) hearing impairment (HI) in Pakistani family DEM4154 was mapped to the *DFNB68* locus (MIM: 610419) on chromosome 19p13.2 with a statistically significant maximum multipoint LOD score of 4.6 (Figure 1A).[9] Family DEM4154 segregates both congenital profound HI and limb malformations but no other abnormalities. Audiometric data obtained from hearing-impaired individual V-4 of family DEM4154 showed profound hearing loss at all frequencies (Figure 1B). Within the mapped region lies *S1PR2* (MIM: 605111), a gene for which knockout mice and zebrafish models were previously shown to have inner ear structural alterations and hearing loss.[3–5,10]

Prior to study onset, approval was obtained from the Institutional Review Boards of the Baylor College of Medicine and Affiliated Hospitals, Combined Neuroscience Institutional Review Board at the NIH, National Centre of Excellence in Molecular Biology, University of the Punjab, and Quaid-I-Azam University. Written informed consent was obtained from all family members who participated in the study. For DEM4154, DNA samples of hearing-impaired individuals V-4 and V-7 (Figure 1A) were

[1]Center for Statistical Genetics, Department of Molecular and Human Genetics, Baylor College of Medicine, Houston, TX 77030, USA; [2]Laboratory of Molecular Genetics, National Institute on Deafness and Other Communication Disorders, NIH, Bethesda, MD 20892, USA; [3]Centre of Excellence in Molecular Biology, University of the Punjab, Lahore 54550, Pakistan; [4]Department of Biochemistry, Faculty of Biological Sciences, Quaid-i-Azam University, Islamabad 45320, Pakistan; [5]Department of Chemistry, Faculty of Natural and Mathematical Sciences, King's College London, London WC2R 2LS, UK; [6]Chandka Medical College, Larkana, Sindh 77150, Pakistan; [7]University of Lahore, Lahore 54550, Pakistan; [8]Department of Biochemistry, Abdul Wali Khan University, Mardan, 23200 Khyber Pakhtunkhwa, Pakistan; [9]Department of Healthcare Biotechnology, Atta-ur-Rahman School of Applied Biosciences (ASAB), National University of Science & Technology (NUST), Islamabad 44000, Pakistan; [10]Department of Biotechnology and Bioinformatics, International Islamic University, Islamabad 44000, Pakistan; [11]Department of Genome Sciences, University of Washington, Seattle, WA 98195, USA; [12]Allama Iqbal Medical Research Centre, Jinnah Hospital Complex, Lahore 54550, Pakistan; [13]Shaheed Zulfiqar Ali Bhutto Medical University, Islamabad 44000, Pakistan
[14]These authors contributed equally to this work
*Correspondence: sleal@bcm.edu
http://dx.doi.org/10.1016/j.ajhg.2015.12.004.

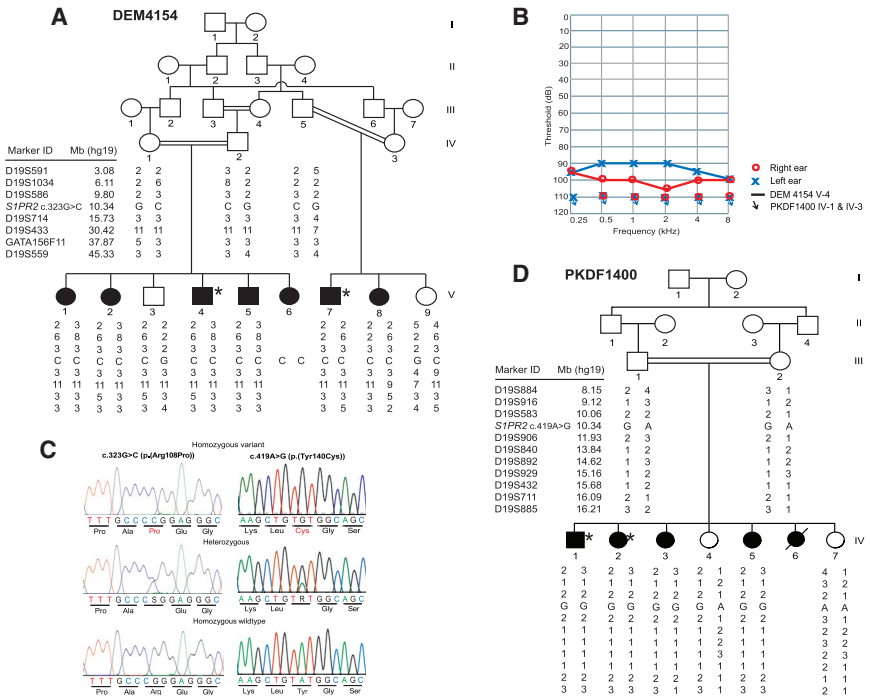

Figure 1. Pedigree Drawings, Mutation Information, and Audiograms for Families with *S1PR2* Variants

(A) Family DEM4154 with the c.323G>C (p.Arg108Pro) variant. Individuals whose DNA samples were submitted for exome sequencing are marked with asterisks. The mapped interval from linkage analysis and homozygosity mapping lies between D19S1034 and D19S433 (6.11–30.42 Mb). Note that a *ZNF91* variant (23.56 Mb) does not segregate with hearing impairment, therefore reducing the mapped interval to 17.45 Mb.

(B) Air-conduction audiograms for individuals V-4 of family DEM4154 (solid lines) and IV-1 and IV-3 of family PKDF1400 (arrows denote residual hearing). Red circles, right ear; blue crosses, left ear. Age (years) at audiometry: 4154 V-4, 20; PKDF1400 IV-1, 19; PKDF1400 IV-3, 12. All three individuals have congenital, profound hearing loss across all frequencies.

(C) Chromatograms comparing an HI individual who is homozygous for each *S1PR2* variant, a heterozygous carrier, and a hearing individual.

(D) Family PKDF1400 with the c.419A>G (p.Tyr140Cys) variant and STR haplotype segregating with hearing impairment. The mapped interval from linkage analysis and homozygosity mapping lies between D19S884 and D19S885 (8.15–16.21 Mb), so the length of the mapped interval is 8.06 Mb.

submitted for exome sequencing at the University of Washington Center for Mendelian Genomics to an average read depth of 77× and 58×, respectively. For both samples, sequence capture was performed in solution with the Roche NimbleGen SeqCap EZ Human Exome Library v.2.0 (~37 Mb target). Fastq files were aligned to the hg19 human reference sequence using Burrows-Wheeler Aligner (BWA)[11] to generate demultiplexed BAM files. Realignment of indel regions, recalibration of base qualities, and variant detection and calling were performed using the Genome Analysis Toolkit (GATK)[12] to produce VCF files. Annotation was performed with SeattleSeq 137.

Rare homozygous variants that are shared by the two hearing-impaired individuals and are predicted to be damaging were identified from exome data using information on genotype status, variant quality control (QC), and annotation from RefSeq, SeattleSeq, dbSNP, the Exome Aggregation Consortium (ExAC), and dbNSFP v.2.9[13] (Table 1). Across the 22 autosomes, only six coding variants were identified to be homozygous in both DEM4154 individuals with HI, passed QC, and had a minor allele frequency (MAF) < 0.01 among South Asian ExAC alleles. All six variants were missense and occurred on chromosome 19, but only three variants occurred within the mapped region and co-segregate with HI (Table 1). Of the three co-segregating variants within 19p13.2, only the c.323G>C (p.Arg108Pro) variant within *S1PR2* (Figures 1A and 1C) was not found in dbSNP and ExAC, occurs at a highly conserved residue, and is predicted to be deleterious in all available bioinformatics results (Table 1). For the *S1PR2* variant, a maximum two-point LOD score[14] of 6.4 was obtained at $\Theta = 0$. A higher LOD score than in the original mapping of *DFNB68* in family DEM4154 was obtained for the *S1PR2* variant due to the very low allele frequency of the variant and the inclusion of an additional family member V-6 (Figure 1A) who was born after the family was initially ascertained. Furthermore, Sanger sequencing of the *S1PR2* c.323G>C variant in 720 Pakistani control chromosomes and our in-house exome sequence data from 76 unrelated Pakistani individuals with non-HI Mendelian phenotypes were both negative for the *S1PR2* variant.

Subsequently, the arHI in another consanguineous family, PKDF1400 (Figure 1D), was mapped to the *DFNB68* region. Multipoint linkage analysis using STR marker genotypes revealed a maximum multipoint LOD score of 3.3 on chromosome 19p13.2–p13.12 (Figure 1D). For this family, a second locus was mapped to chromosome 1q23.3–q25.2 with a multipoint LOD score of 2.1 (data not shown). Audiograms for two hearing-impaired individuals of PKDF1400 both show profound hearing loss across all frequencies (Figure 1B). Careful phenotyping of hearing-impaired individuals ruled out any skeletal, immunologic, cardiovascular, or endocrine features. No history of seizures or vestibular defects was detected in any members of family PKDF1400, further supporting the diagnosis of autosomal-recessive nonsyndromic (ARNS) HI.

For PKDF1400, sequence capture was performed with the Illumina Nextera Rapid Capture Enrichment Kit to create libraries. DNA samples of hearing-impaired siblings IV-1 and IV-2 were exome sequenced at an average depth of 65× and 77×, respectively. Sequence reads were also

Table 1. Homozygous Variants on Chromosome 19 from Exome Data of Families DEM4154 and PKDF1400

Family	DEM4154[a]						PKDF1400[b]	
hg19 Position	9,088,370	10,335,259	13,007,757	23,557,526	36,558,235	38,055,877	9,082,634	10,335,163
Genomic region	19p13.2	19p13.2	19p13.2	19p12	19q13.12	19q13.12	19p13.2	19p13.2
Reference allele	T	C	G	G	G	G	T	T
Alternate allele	G	G	A	A	A	A	C	C
Gene	*MUC16*[c]	*S1PR2*	*GCDH*[d]	*ZNF91*	*WDR62*	*ZNF571*	*MUC16*[c]	*S1PR2*
MIM	606154	605111	608801	603971	613583	NA	606154	605111
GenBank	NM_024690.2	NM_004230.3	NM_000159.3	NM_003430.2	NM_173636.4	NM_016536.3	NM_024690.2	NM_004230.3
cDNA change	c.3445A>C	c.323G>C	c.886G>A	c.71C>T	c.589G>A	c.1453C>T	c.9181A>G	c.419A>G
Amino acid change	p.Thr1149Pro	p.Arg108Pro	p.Gly296Ser	p.Pro24Leu	p.Val197Ile	p.Arg485Cys	p.Met3061Val	p.Tyr140Cys
dbSNP rsID	532389640	NA	539505767	NA	535488873	139005348	571388611	NA
No. ExAC South Asian alleles	62 het, 3 hom	0	61 het, 1 hom	0	31 het	15 het	56 het	0
ExAC South Asian MAF	0.004	0	0.004	0	0.002	0.0002	0.003	0
ExAC all MAF	0.0006	0	0.0006	0	0.0003	0.0001	0.0005	0
MAF in-house exomes (n = 76)	0	0	0.013	0	0	0	0	0
GERP score	−0.4	5.5	5.4	−0.3	5.5	−1.2	−0.5	5.5
phastCons100way_vertebrate	0	1.0	1.0	0.003	1.0	0	0	1.0
phyloP100way_vertebrate	−2.1	7.8	9.5	−1.5	9.3	−2.0	−0.7	6.0
CADD score, scaled	0.9	21.7	21.3	0.002	28.9	11.0	0.001	22.9
Fathmm	tolerated	NA	damaging	tolerated	tolerated	tolerated	tolerated	tolerated
Likelihood ratio test	NA	damaging	damaging	NA	damaging	NA	NA	damaging
Logistic regression (metaLR)	tolerated	damaging	damaging	tolerated	tolerated	tolerated	tolerated	damaging
MutationAssessor	non-functional, neutral	functional, medium	functional, medium	non-functional, neutral	non-functional, low	functional, medium	non-functional, neutral	functional, medium
MutationTaster	NA	disease-causing	disease-causing	polymorphism	disease-causing	polymorphism	polymorphism	disease-causing
PolyPhen2 HVAR	possibly damaging	probably damaging	probably damaging	benign	probably damaging	benign	benign	probably damaging
PROVEAN	neutral	deleterious	deleterious	neutral	neutral	deleterious	neutral	deleterious
SIFT	damaging	damaging	damaging	tolerated	tolerated	tolerated	tolerated	tolerated
Support Vector Machine (metaSVM)	tolerated	damaging	damaging	tolerated	tolerated	tolerated	tolerated	damaging
Segregates with phenotype	yes	yes	yes	no	no	no	yes	yes

Abbreviations are as follows: NA, not available; ExAC, Exome Aggregation Consortium; het, heterozygous; hom, homozygous; MAF, minor allele frequency; CADD, Combined Annotation Dependent Depletion. Conservation scores and bioinformatics results as compiled by dbNSFP v.2.9.

[a]Variants are homozygous in both hearing-impaired individuals V-4 and V-7 of family DEM4154. For either sample, within the mapped interval overall coverage was 99.4%, with median depth of 45×. Coverage at depth ≥15× was 85%.

[b]Variants are homozygous in both hearing-impaired siblings IV-1 and IV-2 from family PKDF1400. For both PKDF1400 samples, 80%–85% of the mapped interval on chr19 was covered by ≥15×.

[c]Although both DEM4154 and PKDF1400 have *MUC16* missense variants, these variants have relatively high MAF in South Asian ExAC alleles, occur at non-conserved residues, and are predicted benign by majority of available bioinformatics results. *MUC16* variants have been identified previously in probands with other Mendelian phenotypes but have been dismissed as non-causal due to the gene's high polymorphic rate.[40]

[d]DEM4154 individuals who are homozygous for the *GCDH* variant do not have signs and symptoms of glutaric aciduria (MIM: 231670). The *GCDH* variant has relatively high South Asian MAF.

mapped against the hg19 human reference sequence using BWA, with recalibration performed using the GATK pipeline. Variant calls were annotated with ANNOVAR. For PKDF1400, within the mapped interval on chromosome 1q23.3–q25.2, no potentially causal variants were identified from exome data. On the other hand, within the mapped interval on chromosome 19p13.2–p13.12, two rare missense variants were shared by the two siblings (Table 1), including *S1PR2* c.419A>G (p.Tyr140Cys). Sanger sequencing revealed that the *S1PR2* variant segregates with HI in family PKDF1400 (Figures 1C and 1D). The c.419A>G (p.Tyr140Cys) variant occurs at a highly conserved residue, is predicted to be deleterious, and is absent in dbSNP and ExAC, in 720 Pakistani control chromosomes, and in 76 Pakistani exomes with non-HI phenotypes, whereas missense variant c.9181A>G (p.Met3061Val) in *MUC16* is present in both ExAC and dbSNP and is predicted to be benign (Table 1). Overall our findings support the contribution of *S1PR2* variants to the etiology of ARNSHI in humans.

Similar to what we observe in humans, *S1pr2*$^{-/-}$ mice had profound deafness as early as postnatal day 22.[3–5] The deafness in mice was believed to be degenerative rather than developmental because of the normal appearance of the inner ear prior to establishment of endocochlear potential and onset of hearing at the end of week 2.[3–5] Histologic analysis of the inner ears of knockout mice demonstrated changes within the stria vascularis by postnatal day 14, and degeneration of hair cells and spiral ganglion neurons and overt signs of inner ear dysfunction were obvious by 3 weeks of age.[3–5] Likewise, in the zebrafish morphant in which translation is inhibited for *milesapart*, a homolog for *S1PR2*, lateral line hair cells were absent or shrunken.[10] Structural defects were also identified within the otic vesicle, the semicircular canals, otoliths, utricle, and saccule of morphant zebrafish.[10] In the *S1pr2*$^{-/-}$ mouse, progressive deterioration of vestibular epithelium and loss or deformity of utricular and saccular otoconia were evident. The utricular otoconia abnormalities were evident as early as P7 prior to manifestation of behavioral balance abnormalities.[3,4] In contrast, saccular otoconia abnormalities became apparent later during adulthood[3,5] and correlated well with the behavioral vestibular defects in *S1pr2*$^{-/-}$ mice as manifested by persistent head tilting and poor swimming ability that became more obvious with age.[3–5] Due to the remote location of families DEM4154 and PKDF1400, reliable documentation by an experienced neurotologist of utricular and saccular function through otolith-ocular reflexes or vestibular evoked myogenic potentials[15] was not available. On the other hand, affected individuals of both families did not present with obvious vestibular symptoms at any age.

The observation of vascular changes in the inner ear prior to cochlear dysfunction is consistent with the role of S1PR2 as a potent regulator of the inflammatory response within vascular endothelium.[16–19] S1PR1 and S1PR2 cooperatively regulate embryonic vascular patterning[20] and endothelial barrier function by influencing the organization of F-actin and tight junction proteins.[21] Dysmorphology of stria vascularis marginal cells and vasculature within the intermediate cell layer of *S1pr2*-deficient mice might indicate the altered function of these cell layers in the establishment of an endocochlear potential.[4] Loss of endocochlear potential, in turn, can lead to deafness and subsequent degeneration of hair cells and spiral ganglion neurons.[3–5] In vitro, activation of S1PR2 is necessary for phosphorylation of ezrin, radixin, and moesin (ERM) proteins that link actin cortical cytoskeleton to the plasma membrane and is therefore important in cellular events that require cytoskeletal rearrangement such as filopodia formation.[22] Interestingly, mutation of radixin results in hearing loss and degeneration of cochlear stereocilia in mice and humans.[23,24] In morphant zebrafish, knockdown of the *S1PR2* homolog resulted in reduced expression of several homologs for genes involved in mouse and human HI, namely *hmx2*, *fgf3*, *pax2*, and *tmie*.[10] Independent mutations in these four downstream genes in mice or humans result in otolith abnormalities, aplastic inner ears, or hair cell defects.[25–28] Taken together, this body of evidence implies that S1PR2 can exert its influence on inner ear function through regulation of inner ear fluid homeostasis or through changes in expression of other essential inner ear proteins.

Within vascular endothelial cells, excess S1P ligand activates S1PR2 and the RhoA/ROCK pathway, resulting in F-actin and tight junction disorganization.[21] Additionally, S1P induces neural progenitor cells to differentiate in the presence of increased S1PR2 expression and phosphorylated MAPK/ERK.[29] To determine whether the identified mutations in the ARNSHI families affect S1PR2 function, a structural model of S1PR2 was predicted with Phyre2[30] and SWISS-MODEL.[31] The X-ray crystal structures of two GPCRs, namely S1PR1[32] (PDB: 3V2W) or the β-2 adrenergic receptor[33] (ADRB2; PDB: 3SN6), were used as templates. Like most GPCRs, S1PRs consist of seven transmembrane helices (TM1–7) and three extracellular loops (ECL1–3).[32] The arginine and glutamic acid residues at positions 108–109 within TM3 at the extracellular side of S1PR2 are identical in S1PRs and similar in GPCRs. Arg120 and Glu121 of S1PR1, which are conserved as Arg108 and Glu109 in S1PR2 (Figure S1A), were previously identified as the most important residues for ligand binding for S1PR1.[32,34,35] Alterations to these two residues led to loss of S1P binding activity and ERK/Akt phosphorylation.[34,35] For S1PR2, Arg108 and Glu109 are predicted to directly interact with S1P, such that Glu109 binds the amide group at the S1P linker while the positively charged guanidino group of Arg108 forms two salt bridges with the negatively charged phosphate head of S1P.[32,34,35] At resting state, Arg108 forms H-bonds with multiple residues, namely Leu92 at the extracellular end of TM2; Thr97, Gln104, and Trp105 within ECL1; and Glu109 of TM3 (Figure S1B). When changed to proline, the residue is instead predicted to form a single H-bond with Ser111

and to lose the side chain that projects into the binding pocket in order to interact with S1P or with ECL1 and TM2 residues (Figure S1B). Based on S1PR1 crystal structure, ECL1 and ECL2 are tightly packed against the N-terminal helix in order to contribute surface area to the ligand-binding pocket and to restrict S1P access, thereby resulting in slow binding saturation when S1P is in excess.[34] The p.Arg108Pro variant would probably affect packing of ECL1 onto the binding pocket, bundling of TM2 against TM3, and proper positioning of Glu109 in order to bind S1P. This suggests that the p.Arg108Pro variant might not only affect direct interaction with S1P, but might also change the structure and properties of the ligand-binding pocket of S1PR2.

Like most GPCRs, extracellular binding of S1P to S1PR2 markedly increases affinity of S1PR2 for G protein from the cytosol. Coupling of S1PR2 with three G proteins is known to initiate signal transduction for several essential pathways: (1) G_i for MAPK/ERK and Akt phosphorylation; (2) G_q for phospholipase C activation; and (3) $G_{12/13}$ for activating the RhoA pathway and also adenylate cyclase for cAMP synthesis.[16] The p.Tyr140Cys variant occurs within intracellular loop 2 (ICL2); based on the known structure of the ADRB2-$G_{\alpha s}$ complex, ICL2 interacts with helices of the G protein and occupies about 25% of buried surface area or interaction points.[33] Additionally, Tyr140 aligns with Tyr141 of ADRB2 (Figure S1A), which is one of three amino acids that facilitate docking of ADRB2 into a hydrophobic pocket of G protein and stabilize the ICL2 helix.[33] For S1PR2, the p.Tyr140Cys variant might result in the gain of an H-bond between Arg130 and Gly141 (Figure S1C). The Arg130 residue within ICL2 of S1PR2 aligns with ADRB2 Arg131 (Figure S1A), which contributes to packing of ICL2 against TM3 and TM7 of the receptor.[33] Loss of the aromatic ring of tyrosine due to the p.Tyr140Cys variant is therefore predicted to interfere with receptor docking and ICL2 stability.

From these modeling predictions, it is hypothesized that *S1PR2* variants result in either loss of activation of S1PR2 by S1P ligand or non-formation of the S1PR2-G protein complex. Both events would result in failed phosphorylation of the MAPK/ERK pathway, which would (1) affect transcription or translation of several inner ear proteins and thereby cause structural defects of the cochlea, otoconia, or hair cells[3–5,10] and (2) result in non-phosphorylation of ERM proteins, which colocalize with S1PR2-activated RhoA in order to maintain tight cell junctions.[21,22] Loss of S1PR2 function is expected to result in inflammation and hyperpermeability of the stria vascularis at onset of hearing function,[21] which can then cause loss of endocochlear potential, hearing loss, and eventually degeneration of inner ear structures.[3–5] Although S1PR2 also induces neural differentiation via phosphorylated MAPK/ERK,[29] knockout mice have apparently normal hair cells and spiral ganglia in the first 2 weeks of life prior to degeneration,[3–5] indicating that failed differentiation of neural cells in the inner ear is not part of the S1PR2 defect.

Previously, the ARNSHI in a second unrelated, consanguineous Pakistani family (DEM4100) was also mapped to the *DFNB68* locus with a maximum multipoint LOD score of 4.8.[9] However, Sanger sequencing revealed no potentially causal variant within *S1PR2*, although a putatively pathogenic variant c.690delT (p.Gly231Valfs*10) was identified in *ESRRB* (MIM: 602167; GenBank: NM_004452.3), a gene that is known to be involved in ARNSHI (Figure S2).[36] This *ESRRB* deletion is predicted to initiate nonsense-mediated decay[37] and is absent in ExAC, 76 in-house exomes, and 174 Pakistani control chromosomes.

For family DEM4154, lower limb deformities were also detected in all hearing-impaired individuals (Figure S3). These limb deformities are not similar to any phenotypes previously observed, with various asymmetric skeletal defects from absence or shortening of leg bones to overlapping, missing, or fused digits. Surprisingly, all the hands of affected individuals appear to have long fingers and possibly fifth digit camptodactyly (Figure S3). It was initially thought that the lower limb deformities do not co-occur with HI due to the lack of obvious deformities in hearing-impaired individual V-7 (Figure 1A). However, X-ray findings of this individual's feet and knees confirmed mild deformities on the right (Figure S3). Gross limb deformities were not observed in family PKDF1400 or *S1pr2*$^{-/-}$ mice, which clearly delineate *S1PR2*'s involvement in ARNSHI. We believe that the limb deformities in family DEM4154 are not due to the *S1PR2* c.323G>C (p.Arg108Pro) variant but are instead due to a variant in another gene. Within the mapped interval, there are ~400 RefSeq genes, but we identified only six coding variants (Table 1) as homozygous in both individuals V-4, who has hearing impairment and severe foot and leg deformities, and V-7, who has hearing impairment and mild foot/knee deformity (Figure S3). Several genes within the mapped interval have been previously associated with limb abnormalities (Table S1), including *EPS15L1*[38] for which exome coverage was incomplete. However, Sanger sequencing of the 5′ UTR and missing coding regions of *EPS15L1* did not reveal potentially causal variants. Across the exome we examined the data for variants that are homozygous in both individuals V-4 and V-7 or homozygous in V-4 but not in V-7 by following up identified variants with Sanger sequencing, but no potentially causal variants were identified. Additionally we did not identify potentially causal variants in genes outside the mapped interval that have been associated with limb defects. Our findings in family DEM4154 demonstrate that not all families with co-occurrence of phenotypes are due to syndromic disease and some warrant investigation to find unique causal variants for each phenotype.

In conclusion, the identification of two unique, deleterious variants within *S1PR2*, each of which segregates with HI in unrelated families, and the occurrence of inner ear abnormalities without other gross malformations in family PKDF1400 or in knockout mice support the involvement of *S1PR2* in ARNSHI. Recently the stonedeaf

(*stdf*) mouse that was homozygous for missense variant *S1pr2* c.866C>G (p.Thr289Arg) was reported to have severe-to-profound hearing impairment, cochlear hair cell loss, changes in the stria vascularis, and reduced endocochlear potential, but no limb abnormalities (K.P. Steel, personal communication). The association of *S1PR2* variants with ARNSHI in humans establishes S1PR2 as an essential inner ear protein and a plausible drug target for inner ear disease. It has been suggested that, in the absence of functional S1PR2, the difference in onset of vascular versus histologic changes in the inner ear presents a "therapeutic window" for selective S1PR2 agonist activity to prevent cochlear degeneration and vestibular deficits in mice.[3,4] However, current evidence indicates multiple functions of S1PR2 by affecting translation or assembly of other proteins that are essential to inner ear function and might imply that the vascular and histologic changes are not sequential but rather are concomitant. Unlike in mice there is no documentation of progressive vestibular deficits in humans with *S1PR2* variants, although congenital deafness begins at fetal stage in humans; therefore, at this point drug targeting of S1PR2-mediated pathways cannot be directly applied to amelioration of genetic inner ear defects. On the other hand, there is evidence in mice that S1P protects against hair cell loss from gentamicin ototoxicity via S1PR2,[39] so it is possible that targeted stimulation of S1PR2 can be used to attenuate the harmful effects of ototoxic drugs on hair cells within the human inner ear.

Accession Numbers

The *SIPR2* variants have been deposited in the ClinVar database under accession numbers SCV000258416 and SCV000258417.

Supplemental Data

Supplemental Data include three figures, one table, and consortium membership and can be found with this article online at http://dx.doi.org/10.1016/j.ajhg.2015.12.004.

Acknowledgments

We are very grateful to the families that participated in this study. This work was supported by NIH intramural funds from the National Institute on Deafness and Other Communication Disorders (NIDCD) DC000039-18 (to T.B.F.), the Higher Education Commission of Pakistan (to S.R. and W.A.), and NIH-NIDCD grants R01 DC011651 and R01 DC003594 (to S.M.L.). Genome-wide genotyping was performed at the Center for Inherited Disease Research, which is funded through the NIH to The Johns Hopkins University, Contract Number N01-HG-65403 (to S.M.L.). Exome sequencing for family DEM4154 was provided by the University of Washington Center for Mendelian Genomics and was funded by the National Human Genome Research Institute and the National Heart, Lung and Blood Institute grant U54HG006493 to D.A.N., Jay Shendure, and M.J.B. Sequencing work for family PKDF1400 utilized the computational resources of the NIH HPC Biowulf cluster.

Received: October 14, 2015
Accepted: December 7, 2015
Published: January 21, 2016

Web Resources

The URLs for data presented herein are as follows:

ANNOVAR, http://annovar.openbioinformatics.org/en/latest/
Burrows-Wheeler Aligner, http://bio-bwa.sourceforge.net/
CADD, http://cadd.gs.washington.edu/
ClinVar, https://www.ncbi.nlm.nih.gov/clinvar/
dbNSFP, https://sites.google.com/site/jpopgen/dbNSFP
dbSNP, http://www.ncbi.nlm.nih.gov/projects/SNP/
ExAC Browser, http://exac.broadinstitute.org/
fathmm v2.3, http://fathmm.biocompute.org.uk/
GATK, https://www.broadinstitute.org/gatk/
HomozygosityMapper software, http://www.homozygositymapper.org/
IGV, http://www.broadinstitute.org/igv/
Likelihood Ratio Test, http://www.genetics.wustl.edu/jflab/lrt_query.html
Mutation Assessor, http://mutationassessor.org/
MutationTaster, http://www.mutationtaster.org/
OMIM, http://www.omim.org/
Phyre2, http://www.sbg.bio.ic.ac.uk/phyre2/html/page.cgi?id=index
PolyPhen-2, http://genetics.bwh.harvard.edu/pph2/
PROVEAN, http://provean.jcvi.org
RCSB Protein Data Bank, http://www.rcsb.org/pdb/home/home.do
SeattleSeq Annotation, http://snp.gs.washington.edu/SeattleSeqAnnotation141/
SWISS-MODEL, http://swissmodel.expasy.org/
UCSC Genome Browser, http://genome.ucsc.edu

References

1. Adada, M., Canals, D., Hannun, Y.A., and Obeid, L.M. (2013). Sphingosine-1-phosphate receptor 2. FEBS J. *280*, 6354–6366.
2. Liu, Y., Wada, R., Yamashita, T., Mi, Y., Deng, C.X., Hobson, J.P., Rosenfeldt, H.M., Nava, V.E., Chae, S.S., Lee, M.J., et al. (2000). Edg-1, the G protein-coupled receptor for sphingosine-1-phosphate, is essential for vascular maturation. J. Clin. Invest. *106*, 951–961.
3. MacLennan, A.J., Benner, S.J., Andringa, A., Chaves, A.H., Rosing, J.L., Vesey, R., Karpman, A.M., Cronier, S.A., Lee, N., Erway, L.C., and Miller, M.L. (2006). The S1P2 sphingosine 1-phosphate receptor is essential for auditory and vestibular function. Hear. Res. *220*, 38–48.
4. Kono, M., Belyantseva, I.A., Skoura, A., Frolenkov, G.I., Starost, M.F., Dreier, J.L., Lidington, D., Bolz, S.S., Friedman, T.B., Hla, T., and Proia, R.L. (2007). Deafness and stria vascularis defects in S1P2 receptor-null mice. J. Biol. Chem. *282*, 10690–10696.
5. Herr, D.R., Grillet, N., Schwander, M., Rivera, R., Müller, U., and Chun, J. (2007). Sphingosine 1-phosphate (S1P) signaling is required for maintenance of hair cells mainly via activation of S1P2. J. Neurosci. *27*, 1474–1478.
6. Ishii, I., Friedman, B., Ye, X., Kawamura, S., McGiffert, C., Contos, J.J., Kingsbury, M.A., Zhang, G., Brown, J.H., and Chun, J. (2001). Selective loss of sphingosine 1-phosphate signaling

with no obvious phenotypic abnormality in mice lacking its G protein-coupled receptor, LP(B3)/EDG-3. J. Biol. Chem. *276*, 33697–33704.
7. Golfier, S., Kondo, S., Schulze, T., Takeuchi, T., Vassileva, G., Achtman, A.H., Gräler, M.H., Abbondanzo, S.J., Wiekowski, M., Kremmer, E., et al. (2010). Shaping of terminal megakaryocyte differentiation and proplatelet development by sphingosine-1-phosphate receptor S1P4. FASEB J. *24*, 4701–4710.
8. Debien, E., Mayol, K., Biajoux, V., Daussy, C., De Aguero, M.G., Taillardet, M., Dagany, N., Brinza, L., Henry, T., Dubois, B., et al. (2013). S1PR5 is pivotal for the homeostasis of patrolling monocytes. Eur. J. Immunol. *43*, 1667–1675.
9. Santos, R.L., Hassan, M.J., Sikandar, S., Lee, K., Ali, G., Martin, P.E., Jr., Wambangco, M.A., Ahmad, W., and Leal, S.M. (2006). DFNB68, a novel autosomal recessive non-syndromic hearing impairment locus at chromosomal region 19p13.2. Hum. Genet. *120*, 85–92.
10. Hu, Z.Y., Zhang, Q.Y., Qin, W., Tong, J.W., Zhao, Q., Han, Y., Meng, J., and Zhang, J.P. (2013). Gene *miles-apart* is required for formation of otic vesicle and hair cells in zebrafish. Cell Death Dis. *4*, e900.
11. Li, H., and Durbin, R. (2009). Fast and accurate short read alignment with Burrows-Wheeler transform. Bioinformatics *25*, 1754–1760.
12. McKenna, A., Hanna, M., Banks, E., Sivachenko, A., Cibulskis, K., Kernytsky, A., Garimella, K., Altshuler, D., Gabriel, S., Daly, M., and DePristo, M.A. (2010). The Genome Analysis Toolkit: a MapReduce framework for analyzing next-generation DNA sequencing data. Genome Res. *20*, 1297–1303.
13. Liu, X., Jian, X., and Boerwinkle, E. (2013). dbNSFP v2.0: a database of human non-synonymous SNVs and their functional predictions and annotations. Hum. Mutat. *34*, E2393–E2402.
14. Fishelson, M., and Geiger, D. (2002). Exact genetic linkage computations for general pedigrees. Bioinformatics *18* (*Suppl 1*), S189–S198.
15. Manzari, L., Burgess, A.M., and Curthoys, I.S. (2010). Dissociation between cVEMP and oVEMP responses: different vestibular origins of each VEMP? Eur. Arch. Otorhinolaryngol. *267*, 1487–1489.
16. Skoura, A., and Hla, T. (2009). Regulation of vascular physiology and pathology by the S1P2 receptor subtype. Cardiovasc. Res. *82*, 221–228.
17. Zhang, W., An, J., Jawadi, H., Siow, D.L., Lee, J.F., Zhao, J., Gartung, A., Maddipati, K.R., Honn, K.V., Wattenberg, B.W., and Lee, M.J. (2013). Sphingosine-1-phosphate receptor-2 mediated NFκB activation contributes to tumor necrosis factor-α induced VCAM-1 and ICAM-1 expression in endothelial cells. Prostaglandins Other Lipid Mediat. *106*, 62–71.
18. Zhao, J., Garcia, D., Gartung, A., and Lee, M.J. (2015). Sphingosine-1-phosphate receptor subtype 2 signaling in endothelial senescence-associated functional impairments and inflammation. Curr. Atheroscler. Rep. *17*, 504.
19. Lorenz, J.N., Arend, L.J., Robitz, R., Paul, R.J., and MacLennan, A.J. (2007). Vascular dysfunction in S1P2 sphingosine 1-phosphate receptor knockout mice. Am. J. Physiol. Regul. Integr. Comp. Physiol. *292*, R440–R446.
20. Mendelson, K., Zygmunt, T., Torres-Vázquez, J., Evans, T., and Hla, T. (2013). Sphingosine 1-phosphate receptor signaling regulates proper embryonic vascular patterning. J. Biol. Chem. *288*, 2143–2156.
21. Li, Q., Chen, B., Zeng, C., Fan, A., Yuan, Y., Guo, X., Huang, X., and Huang, Q. (2015). Differential activation of receptors and signal pathways upon stimulation by different doses of sphingosine-1-phosphate in endothelial cells. Exp. Physiol. *100*, 95–107.
22. Gandy, K.A., Canals, D., Adada, M., Wada, M., Roddy, P., Snider, A.J., Hannun, Y.A., and Obeid, L.M. (2013). Sphingosine 1-phosphate induces filopodia formation through S1PR2 activation of ERM proteins. Biochem. J. *449*, 661–672.
23. Kitajiri, S., Fukumoto, K., Hata, M., Sasaki, H., Katsuno, T., Nakagawa, T., Ito, J., Tsukita, S., and Tsukita, S. (2004). Radixin deficiency causes deafness associated with progressive degeneration of cochlear stereocilia. J. Cell Biol. *166*, 559–570.
24. Khan, S.Y., Ahmed, Z.M., Shabbir, M.I., Kitajiri, S., Kalsoom, S., Tasneem, S., Shayiq, S., Ramesh, A., Srisailpathy, S., Khan, S.N., et al. (2007). Mutations of the RDX gene cause nonsyndromic hearing loss at the DFNB24 locus. Hum. Mutat. *28*, 417–423.
25. Wang, W., Chan, E.K., Baron, S., Van de Water, T., and Lufkin, T. (2001). Hmx2 homeobox gene control of murine vestibular morphogenesis. Development *128*, 5017–5029.
26. Ramsebner, R., Ludwig, M., Parzefall, T., Lucas, T., Baumgartner, W.D., Bodamer, O., Cengiz, F.B., Schoefer, C., Tekin, M., and Frei, K. (2010). A FGF3 mutation associated with differential inner ear malformation, microtia, and microdontia. Laryngoscope *120*, 359–364.
27. Favor, J., Sandulache, R., Neuhäuser-Klaus, A., Pretsch, W., Chatterjee, B., Senft, E., Wurst, W., Blanquet, V., Grimes, P., Spörle, R., and Schughart, K. (1996). The mouse Pax2(1Neu) mutation is identical to a human PAX2 mutation in a family with renal-coloboma syndrome and results in developmental defects of the brain, ear, eye, and kidney. Proc. Natl. Acad. Sci. USA *93*, 13870–13875.
28. Mitchem, K.L., Hibbard, E., Beyer, L.A., Bosom, K., Dootz, G.A., Dolan, D.F., Johnson, K.R., Raphael, Y., and Kohrman, D.C. (2002). Mutation of the novel gene Tmie results in sensory cell defects in the inner ear of spinner, a mouse model of human hearing loss DFNB6. Hum. Mol. Genet. *11*, 1887–1898.
29. Harada, J., Foley, M., Moskowitz, M.A., and Waeber, C. (2004). Sphingosine-1-phosphate induces proliferation and morphological changes of neural progenitor cells. J. Neurochem. *88*, 1026–1039.
30. Kelley, L.A., Mezulis, S., Yates, C.M., Wass, M.N., and Sternberg, M.J. (2015). The Phyre2 web portal for protein modeling, prediction and analysis. Nat. Protoc. *10*, 845–858.
31. Biasini, M., Bienert, S., Waterhouse, A., Arnold, K., Studer, G., Schmidt, T., Kiefer, F., Cassarino, T.G., Bertoni, M., Bordoli, L., and Schwede, T. (2014). SWISS-MODEL: modelling protein tertiary and quaternary structure using evolutionary information. Nucleic Acids Res. *42*, W252–W258.
32. Hanson, M.A., Roth, C.B., Jo, E., Griffith, M.T., Scott, F.L., Reinhart, G., Desale, H., Clemons, B., Cahalan, S.M., Schuerer, S.C., et al. (2012). Crystal structure of a lipid G protein-coupled receptor. Science *335*, 851–855.
33. Rasmussen, S.G., DeVree, B.T., Zou, Y., Kruse, A.C., Chung, K.Y., Kobilka, T.S., Thian, F.S., Chae, P.S., Pardon, E., Calinski, D., et al. (2011). Crystal structure of the β2 adrenergic receptor-Gs protein complex. Nature *477*, 549–555.
34. Parrill, A.L., Wang, D., Bautista, D.L., Van Brocklyn, J.R., Lorincz, Z., Fischer, D.J., Baker, D.L., Liliom, K., Spiegel, S., and Tigyi, G. (2000). Identification of Edg1 receptor residues

that recognize sphingosine 1-phosphate. J. Biol. Chem. *275*, 39379–39384.
35. Jo, E., Sanna, M.G., Gonzalez-Cabrera, P.J., Thangada, S., Tigyi, G., Osborne, D.A., Hla, T., Parrill, A.L., and Rosen, H. (2005). S1P1-selective in vivo-active agonists from high-throughput screening: off-the-shelf chemical probes of receptor interactions, signaling, and fate. Chem. Biol. *12*, 703–715.
36. Collin, R.W., Kalay, E., Tariq, M., Peters, T., van der Zwaag, B., Venselaar, H., Oostrik, J., Lee, K., Ahmed, Z.M., Caylan, R., et al. (2008). Mutations of ESRRB encoding estrogen-related receptor beta cause autosomal-recessive nonsyndromic hearing impairment DFNB35. Am. J. Hum. Genet. *82*, 125–138.
37. Schwarz, J.M., Rödelsperger, C., Schuelke, M., and Seelow, D. (2010). MutationTaster evaluates disease-causing potential of sequence alterations. Nat. Methods *7*, 575–576.
38. Bens, S., Haake, A., Tönnies, H., Vater, I., Stephani, U., Holterhus, P.M., Siebert, R., and Caliebe, A. (2011). A de novo 1.1Mb microdeletion of chromosome 19p13.11 provides indirect evidence for EPS15L1 to be a strong candidate for split hand split foot malformation. Eur. J. Med. Genet. *54*, e501–e504.
39. Nakayama, M., Tabuchi, K., Hoshino, T., Nakamagoe, M., Nishimura, B., and Hara, A. (2014). The influence of sphingosine-1-phosphate receptor antagonists on gentamicin-induced hair cell loss of the rat cochlea. Neurosci. Lett. *561*, 91–95.
40. Ng, S.B., Bigham, A.W., Buckingham, K.J., Hannibal, M.C., McMillin, M.J., Gildersleeve, H.I., Beck, A.E., Tabor, H.K., Cooper, G.M., Mefford, H.C., et al. (2010). Exome sequencing identifies MLL2 mutations as a cause of Kabuki syndrome. Nat. Genet. *42*, 790–793.